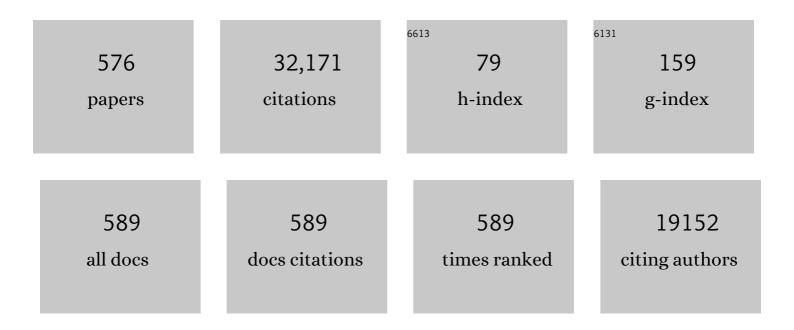


List of Publications by Year in descending order

Source: https://exaly.com/author-pdf/173097/publications.pdf Version: 2024-02-01



#	Article	IF	CITATIONS
1	High-entropy alloy: challenges and prospects. Materials Today, 2016, 19, 349-362.	14.2	1,698
2	Effect of valence electron concentration on stability of fcc or bcc phase in high entropy alloys. Journal of Applied Physics, 2011, 109, .	2.5	1,623
3	Nanostructured surface layer on metallic materials induced by surface mechanical attrition treatment. Materials Science & Engineering A: Structural Materials: Properties, Microstructure and Processing, 2004, 375-377, 38-45.	5.6	913
4	An investigation of surface nanocrystallization mechanism in Fe induced by surface mechanical attrition treatment. Acta Materialia, 2002, 50, 4603-4616.	7.9	897
5	Recent advances for dyes removal using novel adsorbents: A review. Environmental Pollution, 2019, 252, 352-365.	7.5	791
6	Deformation behavior of the Zr41.2Ti13.8Cu12.5Ni10Be22.5 bulk metallic glass over a wide range of strain-rates and temperatures. Acta Materialia, 2003, 51, 3429-3443.	7.9	679
7	Formation of nanostructured surface layer on AISI 304 stainless steel by means of surface mechanical attrition treatment. Acta Materialia, 2003, 51, 1871-1881.	7.9	619
8	Nitriding Iron at Lower Temperatures. Science, 2003, 299, 686-688.	12.6	563
9	Dual-phase nanostructuring as a route to high-strength magnesium alloys. Nature, 2017, 545, 80-83.	27.8	458
10	Plastic strain-induced grain refinement at the nanometer scale in copper. Acta Materialia, 2006, 54, 5281-5291.	7.9	451
11	Fatigue life improvement through surface nanostructuring of stainless steel by means of surface mechanical attrition treatment. Scripta Materialia, 2006, 54, 1949-1954.	5.2	440
12	Microstructure and evolution of mechanically-induced ultrafine grain in surface layer of AL-alloy subjected to USSP. Acta Materialia, 2002, 50, 2075-2084.	7.9	430
13	Ductile fracture: Experiments and computations. International Journal of Plasticity, 2011, 27, 147-180.	8.8	426
14	Nanostructure formation mechanism of α-titanium using SMAT. Acta Materialia, 2004, 52, 4101-4110.	7.9	417
15	Fatigue behaviors of AISI 316L stainless steel with a gradient nanostructured surface layer. Acta Materialia, 2015, 87, 150-160.	7.9	410
16	Surface nanocrystallization of 316L stainless steel induced by ultrasonic shot peening. Materials Science & Engineering A: Structural Materials: Properties, Microstructure and Processing, 2000, 286, 91-95.	5.6	406
17	Tensile properties of a nanocrystalline 316L austenitic stainless steel. Scripta Materialia, 2005, 52, 1039-1044.	5.2	406
18	Atomistic free-volume zones and inelastic deformation of metallic glasses. Nature Materials, 2010, 9, 619-623.	27.5	392

#	Article	IF	CITATIONS
19	Surface nanocrystallization of iron induced by ultrasonic shot peening. Scripta Materialia, 1999, 11, 433-440.	0.5	370
20	Diffusion of chromium in nanocrystalline iron produced by means of surface mechanical attrition treatment. Acta Materialia, 2003, 51, 4319-4329.	7.9	284
21	Effect of surface nanocrystallization on friction and wear properties in low carbon steel. Materials Science & Engineering A: Structural Materials: Properties, Microstructure and Processing, 2003, 352, 144-149.	5.6	277
22	A new method to extract the plastic properties of metal materials from an instrumented spherical indentation loading curve. Acta Materialia, 2004, 52, 4023-4032.	7.9	266
23	Superior adsorption capacity of functionalised straw adsorbent for dyes and heavy-metal ions. Journal of Hazardous Materials, 2020, 382, 121040.	12.4	254
24	Additive manufacturing of structural materials. Materials Science and Engineering Reports, 2021, 145, 100596.	31.8	254
25	The influence of strain rate on the microstructure transition of 304 stainless steel. Acta Materialia, 2011, 59, 3697-3709.	7.9	252
26	Nanostructured Energetic Composites: Synthesis, Ignition/Combustion Modeling, and Applications. ACS Applied Materials & Interfaces, 2014, 6, 3058-3074.	8.0	249
27	Surface nanocrystallization by surface mechanical attrition treatment and its effect on structure and properties of plasma nitrided AISI 321 stainless steel. Acta Materialia, 2006, 54, 5599-5605.	7.9	234
28	Low carbon steel with nanostructured surface layer induced by high-energy shot peening. Scripta Materialia, 2001, 44, 1791-1795.	5.2	225
29	Strain-induced grain refinement of cobalt during surface mechanical attrition treatment. Acta Materialia, 2005, 53, 681-691.	7.9	218
30	Enhanced mechanical behavior of a nanocrystallised stainless steel and its thermal stability. Materials Science & Engineering A: Structural Materials: Properties, Microstructure and Processing, 2007, 445-446, 281-288.	5.6	209
31	Highâ€Strength and Highâ€Ductility Nanostructured and Amorphous Metallic Materials. Advanced Materials, 2014, 26, 5518-5524.	21.0	209
32	Design of high entropy alloys: A single-parameter thermodynamic rule. Scripta Materialia, 2015, 104, 53-55.	5.2	209
33	A review of catalytic performance of metallic glasses in wastewater treatment: Recent progress and prospects. Progress in Materials Science, 2019, 105, 100576.	32.8	209
34	Ultralarge elastic deformation of nanoscale diamond. Science, 2018, 360, 300-302.	12.6	208
35	Modeling grain size dependent optimal twin spacing for achieving ultimate high strength and related high ductility in nanotwinned metals. Acta Materialia, 2011, 59, 5544-5557.	7.9	193
36	Novel cyclodextrin-based adsorbents for removing pollutants from wastewater: A critical review. Chemosphere, 2020, 241, 125043.	8.2	190

#	Article	IF	CITATIONS
37	Efficiently activate peroxymonosulfate by Fe3O4@MoS2 for rapid degradation of sulfonamides. Chemical Engineering Journal, 2021, 422, 130126.	12.7	177
38	Electrochemical doping of anatase TiO ₂ in organic electrolytes for high-performance supercapacitors and photocatalysts. Journal of Materials Chemistry A, 2014, 2, 229-236.	10.3	172
39	Asymmetric flexural behavior from bamboo's functionally graded hierarchical structure: Underlying mechanisms. Acta Biomaterialia, 2015, 16, 178-186.	8.3	171
40	A Novel Multinary Intermetallic as an Active Electrocatalyst for Hydrogen Evolution. Advanced Materials, 2020, 32, e2000385.	21.0	169
41	Bioinspired Simultaneous Changes in Fluorescence Color, Brightness, and Shape of Hydrogels Enabled by AIEgens. Advanced Materials, 2020, 32, e1906493.	21.0	160
42	Origami and 4D printing of elastomer-derived ceramic structures. Science Advances, 2018, 4, eaat0641.	10.3	159
43	Unusual fast secondary relaxation in metallic glass. Nature Communications, 2015, 6, 7876.	12.8	158
44	Metallic Liquids and Glasses: Atomic Order and Global Packing. Physical Review Letters, 2010, 105, 155501.	7.8	157
45	Chromizing behaviors of a low carbon steel processed by means of surface mechanical attrition treatment. Acta Materialia, 2005, 53, 2081-2089.	7.9	154
46	Modelling the plastic deformation of nanostructured metals with bimodal grain size distribution. International Journal of Plasticity, 2012, 30-31, 166-184.	8.8	154
47	Nanostructural metallic materials: Structures and mechanical properties. Materials Today, 2020, 38, 114-135.	14.2	150
48	Optimization of the strain rate to achieve exceptional mechanical properties of 304 stainless steel using high speed ultrasonic surface mechanical attrition treatment. Acta Materialia, 2010, 58, 5086-5096.	7.9	144
49	Polydopamine modified cyclodextrin polymer as efficient adsorbent for removing cationic dyes and Cu2+. Journal of Hazardous Materials, 2020, 389, 121897.	12.4	144
50	Modeling of grain size effect on micro deformation behavior in micro-forming of pure copper. Materials Science & Engineering A: Structural Materials: Properties, Microstructure and Processing, 2010, 527, 6638-6648.	5.6	143
51	Low-temperature nitriding of 38CrMoAl steel with a nanostructured surface layer induced by surface mechanical attrition treatment. Surface and Coatings Technology, 2008, 202, 4957-4963.	4.8	141
52	The size effect on micro deformation behaviour in micro-scale plastic deformation. Materials & Design, 2011, 32, 198-206.	5.1	134
53	Oxygen/Fluorine Dualâ€Doped Porous Carbon Nanopolyhedra Enabled Ultrafast and Highly Stable Potassium Storage. Advanced Functional Materials, 2019, 29, 1906126.	14.9	123
54	Adsorptive removal of bisphenol A, chloroxylenol, and carbamazepine from water using a novel β-cyclodextrin polymer. Ecotoxicology and Environmental Safety, 2019, 170, 278-285.	6.0	120

#	Article	IF	CITATIONS
55	Phase stability and tensile properties of Co-free Al0.5CrCuFeNi2 high-entropy alloys. Journal of Alloys and Compounds, 2014, 584, 530-537.	5.5	116
56	Dislocation evolution in titanium during surface severe plastic deformation. Applied Surface Science, 2009, 255, 6097-6102.	6.1	115
57	Compelling Rejuvenated Catalytic Performance in Metallic Glasses. Advanced Materials, 2018, 30, e1802764.	21.0	115
58	Universal secondary relaxation and unusual brittle-to-ductile transition in metallic glasses. Materials Today, 2017, 20, 293-300.	14.2	114
59	Grain refinement at the nanoscale via mechanical twinning and dislocation interaction in a nickel-based alloy. Journal of Materials Research, 2004, 19, 1623-1629.	2.6	109
60	Nanotwinned and hierarchical nanotwinned metals: a review of experimental, computational and theoretical efforts. Npj Computational Materials, 2018, 4, .	8.7	109
61	The generalized thermodynamic rule for phase selection in multicomponent alloys. Intermetallics, 2015, 59, 75-80.	3.9	108
62	Behavior of air plasma sprayed thermal barrier coatings, subject to intense thermal cycling. Surface and Coatings Technology, 2003, 166, 37-43.	4.8	105
63	A study of the process and kinetics of electrochemical deposition and the hydrothermal synthesis of hydroxyapatite coatings. Journal of Materials Science: Materials in Medicine, 2000, 11, 667-673.	3.6	104
64	Thermal cyclic behavior of air plasma sprayed thermal barrier coatings sprayed on stainless steel substrates. Surface and Coatings Technology, 2007, 201, 4653-4658.	4.8	99
65	Characterization and stability of hydroxyapatite coatings prepared by an electrodeposition and alkaline-treatment process. Journal of Biomedical Materials Research Part B, 2001, 54, 96-101.	3.1	97
66	Hierarchical nanostructured aluminum alloy with ultrahigh strength and large plasticity. Nature Communications, 2019, 10, 5099.	12.8	97
67	Fabrication of nickel oxide-embedded titania nanotube array for redox capacitance application. Electrochimica Acta, 2008, 53, 3643-3649.	5.2	95
68	Literature review on the mechanical properties of materials after surface mechanical attrition treatment (SMAT). Nano Materials Science, 2020, 2, 3-31.	8.8	94
69	Development of Nanostructures in Metallic Materials with Low Stacking Fault Energies During Surface Mechanical Attrition Treatment (SMAT). Materials Transactions, 2003, 44, 1919-1925.	1.2	93
70	Atomic-Scale Structural Evolution and Stability of Supercooled Liquid of a Zr-Based Bulk Metallic Glass. Physical Review Letters, 2011, 106, 215505.	7.8	93
71	Effect of residual stresses on air plasma sprayed thermal barrier coatings. Surface and Coatings Technology, 2003, 168, 291-299.	4.8	89
72	A Selfâ€Supported Highâ€Entropy Metallic Glass with a Nanosponge Architecture for Efficient Hydrogen Evolution under Alkaline and Acidic Conditions. Advanced Functional Materials, 2021, 31, 2101586.	14.9	89

#	Article	IF	CITATIONS
73	Determination of Residual Stress in Composite Laminates Using the Incremental Hole-drilling Method. Journal of Composite Materials, 2003, 37, 831-844.	2.4	87
74	Wear and corrosion properties of a low carbon steel processed by means of SMAT followed by lower temperature chromizing treatment. Surface and Coatings Technology, 2006, 201, 2796-2801.	4.8	87
75	Gradient twinned 304 stainless steels for high strength and high ductility. Materials Science & Engineering A: Structural Materials: Properties, Microstructure and Processing, 2016, 667, 179-188.	5.6	87
76	Microstructures-based constitutive analysis for mechanical properties of gradient-nanostructured 304 stainless steels. Acta Materialia, 2017, 128, 375-390.	7.9	86
77	High-order hierarchical nanotwins with superior strength and ductility. Acta Materialia, 2018, 149, 397-406.	7.9	85
78	Recent advances and prospects of persistent luminescent materials as inner secondary self-luminous light source for photocatalytic applications. Chemical Engineering Journal, 2021, 403, 126099.	12.7	84
79	Influence of size effect on the springback of sheet metal foils in micro-bending. Computational Materials Science, 2011, 50, 2604-2614.	3.0	83
80	Fe _{1â^'x} S/C nanocomposites from sugarcane waste-derived microporous carbon for high-performance lithium ion batteries. Green Chemistry, 2016, 18, 3029-3039.	9.0	83
81	Mechanical properties and thermal stability of nanocrystallized pure aluminum produced by surface mechanical attrition treatment. Materials Science & Engineering A: Structural Materials: Properties, Microstructure and Processing, 2015, 636, 446-451.	5.6	82
82	Measurement of residual-stress distribution by the incremental hole-drilling method. Experimental Mechanics, 1985, 25, 175-185.	2.0	80
83	Nano-scratch and fretting wear study of DLC coatings for biomedical application. Diamond and Related Materials, 2001, 10, 1448-1456.	3.9	79
84	Fiber Bragg gratings with enhanced thermal stability by residual stress relaxation. Optics Express, 2009, 17, 19785.	3.4	78
85	Self-ordered Nanotubular TiO2 Multilayers for High-Performance Photocatalysts and Supercapacitors. Electrochimica Acta, 2016, 203, 257-264.	5.2	78
86	Dislocation activities at the martensite phase transformation interface in metastable austenitic stainless steel: An in-situ TEM study. Materials Science & Engineering A: Structural Materials: Properties, Microstructure and Processing, 2017, 703, 236-243.	5.6	78
87	Superior Tensile Ductility in Bulk Metallic Glass with Gradient Amorphous Structure. Scientific Reports, 2014, 4, 4757.	3.3	77
88	Highly Exothermic and Superhydrophobic Mg/Fluorocarbon Core/Shell Nanoenergetic Arrays. ACS Applied Materials & Interfaces, 2014, 6, 10497-10505.	8.0	76
89	Dramatic enhancement effects of l-cysteine on the degradation of sulfadiazine in Fe3+/CaO2 system. Journal of Hazardous Materials, 2020, 383, 121133.	12.4	76
90	Enhanced mechanical properties and corrosion resistance of 316L stainless steel by pre-forming a gradient nanostructured surface layer and annealing. Acta Materialia, 2021, 208, 116773.	7.9	76

#	Article	IF	CITATIONS
91	γ→ε martensite transformation and twinning deformation in fcc cobalt during surface mechanical attrition treatment. Scripta Materialia, 2005, 52, 547-551.	5.2	75
92	Make nanostructured metal exceptionally tough by introducing non-localized fracture behaviors. Scripta Materialia, 2008, 59, 579-582.	5.2	75
93	Alumina grit blasting parameters for surface preparation in the plasma spraying operation. Journal of Thermal Spray Technology, 1997, 6, 217-227.	3.1	74
94	Analysis of the twin spacing and grain size effects on mechanical properties in hierarchically nanotwinned face-centered cubic metals based on a mechanism-based plasticity model. Journal of the Mechanics and Physics of Solids, 2015, 76, 162-179.	4.8	74
95	Attractive In Situ Selfâ€Reconstructed Hierarchical Gradient Structure of Metallic Glass for High Efficiency and Remarkable Stability in Catalytic Performance. Advanced Functional Materials, 2019, 29, 1807857.	14.9	74
96	Fe3O4/graphene aerogels: A stable and efficient persulfate activator for the rapid degradation of malachite green. Chemosphere, 2020, 251, 126402.	8.2	74
97	Surface Nanocrystallization by Surface Mechanical Attrition Treatment. Materials Science Forum, 0, 579, 91-108.	0.3	71
98	One-dimensional CuO nanowire: synthesis, electrical, and optoelectronic devices application. Nanoscale Research Letters, 2014, 9, 637.	5.7	71
99	Low-temperature fabrication of brown TiO ₂ with enhanced photocatalytic activities under visible light. Chemical Communications, 2016, 52, 2988-2991.	4.1	71
100	Strain Engineering of Metal Halide Perovskites on Coupling Anisotropic Behaviors. Advanced Functional Materials, 2021, 31, 2006243.	14.9	71
101	Effects of specimen geometry and base material on the mechanical behavior of focused-ion-beam-fabricated metallic-glass micropillars. Acta Materialia, 2009, 57, 1613-1623.	7.9	70
102	The atomic-scale mechanism for the enhanced glass-forming-ability of a Cu-Zr based bulk metallic glass with minor element additions. Scientific Reports, 2014, 4, 4648.	3.3	70
103	Interface evolution of Si/Mullite/Yb2SiO5 PS-PVD environmental barrier coatings under high temperature. Journal of the European Ceramic Society, 2020, 40, 1478-1487.	5.7	70
104	Viscoelastic creep and relaxation of dielectric elastomers characterized by a Kelvin-Voigt-Maxwell model. Applied Physics Letters, 2017, 110, .	3.3	68
105	Rare earth-free composites of carbon dots/metal–organic frameworks as white light emitting phosphors. Journal of Materials Chemistry C, 2019, 7, 2207-2211.	5.5	68
106	Construction of FeP Hollow Nanoparticles Densely Encapsulated in Carbon Nanosheet Frameworks for Efficient and Durable Electrocatalytic Hydrogen Production. Advanced Science, 2019, 6, 1801490.	11.2	68
107	Ballistic performance of nanocrystalline and nanotwinned ultrafine crystal steel. Acta Materialia, 2012, 60, 1353-1367.	7.9	66
108	Crystal–Glass Highâ€Entropy Nanocomposites with Near Theoretical Compressive Strength and Large Deformability. Advanced Materials, 2020, 32, e2002619.	21.0	66

#	Article	IF	CITATIONS
109	Morphology and composition of hydroxyapatite coatings prepared by hydrothermal treatment on electrodeposited brushite coatings. Journal of Materials Science: Materials in Medicine, 1999, 10, 243-248.	3.6	65
110	Nanomechanical properties of nanostructured titanium prepared by SMAT. Surface and Coatings Technology, 2006, 201, 208-213.	4.8	65
111	Degradation of sulfanilamide by Fenton-like reaction and optimization using response surface methodology. Ecotoxicology and Environmental Safety, 2019, 172, 334-340.	6.0	65
112	Wear behavior of nanocrystalline structured magnesium alloy induced by surface mechanical attrition treatment. Surface and Coatings Technology, 2015, 261, 219-226.	4.8	64
113	Measurement of residual-stress distribution by the incremental hole-drilling method. Journal of Mechanical Working Technology, 1985, 11, 167-188.	0.1	62
114	The formation of ε-Fe3–2N phase in a nanocrystalline Fe. Scripta Materialia, 2004, 50, 647-650.	5.2	62
115	Small punch testing for assessing the fracture properties of the reactor vessel steel with different thicknesses. Nuclear Engineering and Design, 2008, 238, 3186-3193.	1.7	62
116	Improving the intergranular corrosion resistance of austenitic stainless steel by high density twinned structure. Scripta Materialia, 2017, 130, 264-268.	5.2	61
117	The deformation behavior of AZ31 Mg alloy with surface mechanical attrition treatment. Materials Science & Engineering A: Structural Materials: Properties, Microstructure and Processing, 2017, 707, 636-646.	5.6	61
118	CuO/Mg/fluorocarbon sandwich-structure superhydrophobic nanoenergetic composite with anti-humidity property. Chemical Engineering Journal, 2015, 266, 163-170.	12.7	60
119	Pt nanoparticles decorated heterostructured g-C3N4/Bi2MoO6 microplates with highly enhanced photocatalytic activities under visible light. Scientific Reports, 2019, 9, 7636.	3.3	60
120	Fatigue strength improvement of selective laser melted Ti6Al4V using ultrasonic surface mechanical attrition. Materials Research Letters, 2019, 7, 327-333.	8.7	60
121	Influence of experimental parameters on determination of residual stress using the incremental hole-drilling method. Composites Science and Technology, 2004, 64, 171-180.	7.8	59
122	An energy-based method to extract plastic properties of metal materials from conical indentation tests. Journal of Materials Research, 2005, 20, 1194-1206.	2.6	59
123	The tensile properties of titanium processed by surface mechanical attrition treatment. Surface and Coatings Technology, 2008, 202, 4728-4733.	4.8	59
124	Study of Residual Stress Distribution by a Combined Method of Moire´ Interferometry and Incremental Hole Drilling, Part I: Theory. Journal of Applied Mechanics, Transactions ASME, 1998, 65, 837-843.	2.2	58
125	Study of the performance of different subpixel image correlation methods in 3D digital image correlation. Applied Optics, 2010, 49, 4044.	2.1	58
126	Microstructure evolution and mechanical properties of an Mg–Gd alloy subjected to surface mechanical attrition treatment. Materials Science & Engineering A: Structural Materials: Properties, Microstructure and Processing, 2015, 630, 146-154.	5.6	58

#	Article	IF	CITATIONS
127	An experimental study of residual stress induced by ultrasonic shot peening. Journal of Materials Processing Technology, 2004, 152, 56-61.	6.3	57
128	A statistical model for predicting the mechanical properties of nanostructured metals with bimodal grain size distribution. Acta Materialia, 2012, 60, 5762-5772.	7.9	57
129	Fracture Morphology and Quenched-in Precipitates Induced Embrittlement in a Zr-base Bulk Glass. Materials Transactions, 2001, 42, 356-364.	1.2	56
130	Strengthening and toughening by interface-mediated slip transfer reaction in nanotwinned copper. Scripta Materialia, 2009, 60, 508-511.	5.2	56
131	Error evaluation technique for three-dimensional digital image correlation. Applied Optics, 2011, 50, 6239.	2.1	56
132	An innovative Mg/Ti hybrid fixation system developed for fracture fixation and healing enhancement at load-bearing skeletal site. Biomaterials, 2018, 180, 173-183.	11.4	55
133	Dramatic improvement enabled by incorporating thermal conductive TiN into Si-based anodes for lithium ion batteries. Energy Storage Materials, 2020, 29, 367-376.	18.0	55
134	Simulation-enabled study of folding defect formation and avoidance in axisymmetrical flanged components. Journal of Materials Processing Technology, 2009, 209, 5077-5086.	6.3	53
135	Facile Green In Situ Synthesis of Mg/CuO Core/Shell Nanoenergetic Arrays with a Superior Heat-Release Property and Long-Term Storage Stability. ACS Applied Materials & Interfaces, 2013, 5, 7641-7646.	8.0	53
136	A novel L12-strengthened multicomponent Co-rich high-entropy alloy with both high γ′-solvus temperature and superior high-temperature strength. Scripta Materialia, 2021, 199, 113826.	5.2	53
137	Microstructural evolution and formation of nanocrystalline intermetallic compound during surface mechanical attrition treatment of cobalt. Acta Materialia, 2007, 55, 5768-5779.	7.9	52
138	Corrosion behavior on orthopedic NiTi alloy with nanocrystalline/amorphous surface. Materials Chemistry and Physics, 2011, 126, 102-107.	4.0	52
139	Experimental and simulation study of deformation behavior in micro-compound extrusion process. Materials & Design, 2011, 32, 525-534.	5.1	52
140	The effects and mechanisms of zero-valent iron on anaerobic digestion of solid waste: A mini-review. Journal of Cleaner Production, 2021, 278, 123567.	9.3	52
141	Extraction of bulk metallic-glass yield strengths using tapered micropillars in micro-compression experiments. Intermetallics, 2010, 18, 385-393.	3.9	51
142	Facile fabrication of N/S-doped carbon nanotubes with Fe ₃ O ₄ nanocrystals enchased for lasting synergy as efficient oxygen reduction catalysts. Journal of Materials Chemistry A, 2017, 5, 13189-13195.	10.3	50
143	Improved nitrogen transport in surface nanocrystallized low-carbon steels during gaseous nitridation. Materials Letters, 2002, 55, 340-343.	2.6	49
144	Thermal and Nonthermal Effects in Plasmonâ€Mediated Electrochemistry at Nanostructured Ag Electrodes. Angewandte Chemie - International Edition, 2020, 59, 6790-6793.	13.8	49

#	Article	IF	CITATIONS
145	Study of the intrinsic ductile to brittle transition mechanism of metallic glasses. Acta Materialia, 2009, 57, 6037-6046.	7.9	48
146	Tuning the Bi ³⁺ -photoemission color over the entire visible region by manipulating secondary cations modulation in the ScV _x P _{1â^x} O ₄ :Bi ³⁺ (0 ≤i>x ≤) solid solution. Journal of Materials Chemistry C, 2019, 7, 9865-9877.	5.5	48
147	Residual stresses in laser welded aluminium plate by use of ultrasonic and optical methods. Materials Science & Engineering A: Structural Materials: Properties, Microstructure and Processing, 2004, 382, 257-264.	5.6	47
148	Nature-Inspired Hierarchical Steels. Scientific Reports, 2018, 8, 5088.	3.3	47
149	Multicolor Tuning and Temperature-Triggered Anomalous Eu ³⁺ -Related Photoemission Enhancement via Interplay of Accelerated Energy Transfer and Release of Defect-Trapped Electrons in the Tb ³⁺ ,Eu ³⁺ -Doped Strontium–Aluminum Chlorites. ACS Applied Materials &: Interfaces. 2018. 10. 36157-36170.	8.0	47
150	A Facile Strategy to Construct Silverâ€Modified, ZnOâ€Incorporated and Carbonâ€Coated Silicon/Porousâ€Carbon Nanofibers with Enhanced Lithium Storage. Small, 2019, 15, e1900436.	10.0	47
151	Theory of designing the gradient microstructured metals for overcoming strength-ductility trade-off. Scripta Materialia, 2020, 184, 41-45.	5.2	47
152	Electrical reliability aspects of HfO2 high-k gate dielectrics with TaN metal gate electrodes under constant voltage stress. Microelectronics Reliability, 2006, 46, 69-76.	1.7	46
153	Elemental segregation in solid-solution high-entropy alloys: Experiments and modeling. Journal of Alloys and Compounds, 2016, 681, 167-174.	5.5	46
154	Influence of rolling temperature on microstructural evolution and mechanical behavior of AZ31 alloy with accumulative roll bonding. Materials Science & Engineering A: Structural Materials: Properties, Microstructure and Processing, 2019, 754, 112-120.	5.6	46
155	Study of residual stress in surface nanostructured AISI 316L stainless steel using two mechanical methods. Surface and Coatings Technology, 2003, 168, 148-155.	4.8	45
156	Photoelectrochemical behavior of titania nanotube array grown on nanocrystalline titanium. Journal of Materials Science, 2009, 44, 2907-2915.	3.7	45
157	Micromechanical simulation of fracture behavior of bimodal nanostructured metals. Materials Science & Engineering A: Structural Materials: Properties, Microstructure and Processing, 2014, 618, 479-489.	5.6	45
158	Combining gradient structure and supersaturated solid solution to achieve superior mechanical properties in WE43 magnesium alloy. Journal of Materials Science and Technology, 2022, 99, 223-238.	10.7	45
159	On the role of hierarchical twins for achieving maximum yield strength in nanotwinned metals. Applied Physics Letters, 2012, 101, 081906.	3.3	44
160	Sol-gel derived TiO2 coating on plasma nitrided 316L stainless steel. Vacuum, 2012, 86, 1402-1407.	3.5	44
161	Study of Residual Stress Distribution by a Combined Method of Moire´Interferometry and Incremental Hole Drilling, Part II: Implementation. Journal of Applied Mechanics, Transactions ASME, 1998, 65, 844-850.	2.2	43
162	Analysis of nano-scratch behavior of diamond-like carbon films. Surface and Coatings Technology, 2002, 154, 232-236.	4.8	43

#	Article	IF	CITATIONS
163	Fluid–structure interaction of single flexible cylinder in axial flow. Computers and Fluids, 2012, 56, 143-151.	2.5	43
164	Effects of surface nanocrystallization on the corrosion behaviors of 316L and alloy 690. Surface and Coatings Technology, 2017, 309, 227-231.	4.8	43
165	Defective Black TiO ₂ Nanotube Arrays for Enhanced Photocatalytic and Photoelectrochemical Applications. ACS Applied Nano Materials, 2019, 2, 7372-7378.	5.0	43
166	Lamellarly Stacking Porous N, P Coâ€Doped Mo ₂ C/C Nanosheets as High Performance Anode for Lithiumâ€lon Batteries. Small, 2019, 15, e1805022.	10.0	43
167	Anodic Synthesis of Hierarchical SnS/SnO <i>_x</i> Hollow Nanospheres and Their Application for Highâ€Performance Naâ€Ion Batteries. Advanced Functional Materials, 2019, 29, 1901000.	14.9	43
168	A new method for evaluating the scratch resistance of diamond-like carbon films by the nano-scratch technique. Diamond and Related Materials, 2002, 11, 1454-1459.	3.9	41
169	Strain rate measurement by Electronic Speckle Pattern Interferometry: A new look at the strain localization onset. Materials Science & Engineering A: Structural Materials: Properties, Microstructure and Processing, 2006, 415, 234-241.	5.6	41
170	Development of Bioimplants with 2D, 3D, and 4D Additive Manufacturing Materials. Engineering, 2020, 6, 1232-1243.	6.7	41
171	Effect of surface mechanical attrition treatment on corrosion fatigue behavior of AZ31B magnesium alloy. International Journal of Fatigue, 2019, 127, 461-469.	5.7	40
172	Facile Synthesis of Nitrogenâ€Rich Carbon Dots as Fertilizers for Mung Bean Sprouts. Advanced Sustainable Systems, 2019, 3, 1800132.	5.3	40
173	The influences of heat treatments and interdiffusion on the adhesion of plasma-sprayed NiCrAlY coatings. Surface and Coatings Technology, 1996, 82, 99-109.	4.8	39
174	Determination of residual stress using critically refracted longitudinal waves and immersion mode. Journal of Strain Analysis for Engineering Design, 2002, 37, 13-20.	1.8	39
175	Localized solid-state amorphization at grain boundaries in a nanocrystalline Al solid solution subjected to surface mechanical attrition. Journal Physics D: Applied Physics, 2005, 38, 4140-4143.	2.8	39
176	A 3D brick element based on Hu-Washizu variational principle for mesh distortion. International Journal for Numerical Methods in Engineering, 2002, 53, 2529-2548.	2.8	38
177	First-principles Calculations of Strengthening Compounds in Magnesium Alloy: A General Review. Journal of Materials Science and Technology, 2016, 32, 1222-1231.	10.7	38
178	Effect of Surface Mechanical Attrition Treatment on Tribological Behavior of the AZ31 Alloy. Journal of Materials Science and Technology, 2016, 32, 1245-1252.	10.7	38
179	Construction of MoO ₂ Quantum Dot–Graphene and MoS ₂ Nanoparticle–Graphene Nanoarchitectures toward Ultrahigh Lithium Storage Capability. ACS Applied Materials & Interfaces, 2017, 9, 28441-28450.	8.0	38
180	Development of the high-precision incremental-step hole-drilling method for the study of residual stress in multi-layer materials: influence of temperature and substrate on ZrO2–Y2O3 8 wt.% coatings. Surface and Coatings Technology, 2002, 155, 152-160.	4.8	37

#	Article	IF	CITATIONS
181	Propagation of exchange bias in CoFeâ^•FeMnâ^•CoFe trilayers. Applied Physics Letters, 2008, 93, .	3.3	37
182	High strength and high ductility copper obtained by topologically controlled planar heterogeneous structures. Scripta Materialia, 2016, 124, 103-107.	5.2	37
183	Microstructure Evolution and Mechanical Properties of a SMATed Mg Alloy under In Situ SEM Tensile Testing. Journal of Materials Science and Technology, 2017, 33, 224-230.	10.7	37
184	Enhanced Corrosion Properties of Nanostructured 316 Stainless Steel in 0.6ÂM NaCl Solution. Journal of Bio- and Tribo-Corrosion, 2019, 5, 1.	2.6	37
185	A novel hollow-sphere cyclodextrin nanoreactor for the enhanced removal of bisphenol A under visible irradiation. Journal of Hazardous Materials, 2020, 384, 121267.	12.4	37
186	Evaluation of scratch resistance of diamond-like carbon films on Ti alloy substrate by nano-scratch technique. Diamond and Related Materials, 2002, 11, 1505-1510.	3.9	36
187	Evaluation of nanostructured carbonated hydroxyapatite coatings formed by a hybrid process of plasma spraying and hydrothermal synthesis. Journal of Biomedical Materials Research Part B, 2002, 60, 511-516.	3.1	36
188	Cooling rate effect on Young's modulus and hardness of a Zr-based metallic glass. Journal of Alloys and Compounds, 2011, 509, 3269-3273.	5.5	36
189	Short-circuit diffusion growth of long bi-crystal CuO nanowires. Chemical Physics Letters, 2011, 504, 41-45.	2.6	36
190	Mechanical properties of DLC coating sputter deposited on surface nanocrystallized 304 stainless steel. Surface and Coatings Technology, 2012, 207, 555-564.	4.8	36
191	Methodology for the evaluation of yield strength and hardening behavior of metallic materials by indentation with spherical tip. Journal of Applied Physics, 2003, 94, 288-294.	2.5	35
192	A novel structural gradient metallic glass composite with enhanced mechanical properties. Scripta Materialia, 2009, 61, 608-611.	5.2	35
193	The main factor influencing the tensile properties of surface nano-crystallized graded materials. Materials Science & Engineering A: Structural Materials: Properties, Microstructure and Processing, 2010, 527, 7040-7044.	5.6	35
194	A new constitutive model for shear banding instability in metallic glass. International Journal of Solids and Structures, 2011, 48, 3112-3127.	2.7	35
195	Chemically dealloyed Fe-based metallic glass with void channels-like architecture for highly enhanced peroxymonosulfate activation in catalysis. Journal of Alloys and Compounds, 2019, 785, 642-650.	5.5	35
196	An integrated FEM and ANN methodology for metal-formed product design. Engineering Applications of Artificial Intelligence, 2008, 21, 1170-1181.	8.1	34
197	First-principles prediction and experimental verification of glass-forming ability in Zr-Cu binary metallic glasses. Scientific Reports, 2013, 3, 2124.	3.3	34
198	Enhanced Passivation Layer by Cr Diffusion of 301 Stainless Steel Facilitated by SMAT. Advanced Engineering Materials, 2019, 21, 1900125.	3.5	34

#	Article	lF	CITATIONS
199	Perovskite Core–Shell Nanowire Transistors: Interfacial Transfer Doping and Surface Passivation. ACS Nano, 2020, 14, 12749-12760.	14.6	34
200	Carbon Nanotubes for Space and Bio-Engineering Applications. Journal of Computational and Theoretical Nanoscience, 2008, 5, 23-35.	0.4	33
201	Wear resistance of NiTi alloy after surface mechanical attrition treatment. Surface and Coatings Technology, 2010, 205, 506-510.	4.8	33
202	Effect of surface modifications on shear banding and plasticity in metallic glasses: An overview. Progress in Natural Science: Materials International, 2012, 22, 355-363.	4.4	33
203	A Dynamic Model of Chemoattractant-Induced Cell Migration. Biophysical Journal, 2015, 108, 1645-1651.	0.5	33
204	Mesoporous C-coated SnO _x nanosheets on copper foil as flexible and binder-free anodes for superior sodium-ion batteries. Journal of Materials Chemistry A, 2017, 5, 2243-2250.	10.3	33
205	Gold Nanoparticle-Decorated Silver Needle for Surface-Enhanced Raman Spectroscopy Screening of Residual Malachite Green in Aquaculture Products. ACS Applied Nano Materials, 2019, 2, 2752-2757.	5.0	33
206	UiO-66-NO ₂ as an Oxygen "Pump―for Enhancing Oxygen Reduction Reaction Performance. Chemistry of Materials, 2019, 31, 1646-1654.	6.7	33
207	A new scheme for computational modeling of conical indentation in plastically graded materials. Journal of Materials Research, 2004, 19, 1703-1716.	2.6	32
208	Elasto-plastic deformation and fracture mechanism of a diamond-like carbon film deposited on a Ti–6Al–4V substrate in nano-scratch test. Thin Solid Films, 2004, 466, 175-182.	1.8	32
209	Low-temperature plasma nitriding of AISI 304 stainless steel with nano-structured surface layer. International Journal of Materials Research, 2003, 94, 1143-1147.	0.8	31
210	Geometrical modeling of granular structures in two and three dimensions. Application to nanostructures. International Journal for Numerical Methods in Engineering, 2009, 80, 425-454.	2.8	31
211	Structural inhomogeneity and anelastic deformation in metallic glasses revealed by spherical nanoindentation. Applied Physics Letters, 2010, 97, .	3.3	31
212	Characteristic length scales governing plasticity/brittleness of bulk metallic glasses at ambient temperature. Applied Physics Letters, 2010, 96, 011905.	3.3	31
213	Evolution of texture and microstructure in pulsed electro-deposited Cu treated by Surface Mechanical Attrition Treatment (SMAT). Journal of Alloys and Compounds, 2010, 504, S410-S413.	5.5	31
214	High-performance supercapacitors based on amorphous C-modified anodic TiO2 nanotubes. Applied Surface Science, 2016, 362, 399-405.	6.1	31
215	Enhanced mechanical properties of Ti6Al4V alloy fabricated by laser additive manufacturing under static magnetic field. Materials Research Letters, 2022, 10, 530-538.	8.7	31
216	Manipulation of air plasma spraying parameters for the production of ceramic coatings. Journal of Materials Processing Technology, 2009, 209, 2508-2514.	6.3	30

#	Article	IF	CITATIONS
217	Numerical simulation of the fluid–structure interaction for an elastic cylinder subjected to tubular fluid flow. Computers and Fluids, 2012, 68, 192-202.	2.5	30
218	Water-enabled crystallization of mesoporous SnO ₂ as a binder-free electrode for enhanced sodium storage. Journal of Materials Chemistry A, 2017, 5, 23967-23975.	10.3	30
219	Static and dynamic mechanical behaviors of gradient-nanotwinned stainless steel with a composite structure: Experiments and modeling. International Journal of Plasticity, 2019, 114, 272-288.	8.8	30
220	Accelerated photoelectron transmission by carboxymethyl β-cyclodextrin for organic contaminants removal: An alternative to noble metal catalyst. Journal of Hazardous Materials, 2020, 393, 122414.	12.4	30
221	A Review of Recent Developments and Applications in the Field of X-Ray Diffraction for Residual Stress Studies. Journal of Strain Analysis for Engineering Design, 1998, 33, 127-136.	1.8	30
222	Study of through-thickness residual stress by numerical and experimental techniques. Journal of Strain Analysis for Engineering Design, 1998, 33, 449-458.	1.8	29
223	A precise correcting method for the study of the superhard material using nanoindentation tests. Journal of Materials Research, 2007, 22, 1255-1264.	2.6	29
224	Microindentation as a local damage measurement technique. Materials Letters, 2007, 61, 34-36.	2.6	29
225	Investigation of non-local cracking in layered stainless steel with nanostructured interface. Scripta Materialia, 2010, 63, 403-406.	5.2	29
226	Scale law of complex deformation transitions of nanotwins in stainless steel. Nature Communications, 2019, 10, 1403.	12.8	29
227	Massive interstitial solid solution alloys achieve near-theoretical strength. Nature Communications, 2022, 13, 1102.	12.8	29
228	An inverse approach for constructing the residual stress field induced by welding. Journal of Strain Analysis for Engineering Design, 2002, 37, 345-359.	1.8	28
229	Heat treatment of thermal barrier coatings. Materials Science & Engineering A: Structural Materials: Properties, Microstructure and Processing, 2003, 359, 129-136.	5.6	28
230	Residual stresses measurement by using ring-core method and 3D digital image correlation technique. Measurement Science and Technology, 2013, 24, 085604.	2.6	28
231	The Portevin-Le Châtelier effect of gradient nanostructured 5182 aluminum alloy by surface mechanical attrition treatment. Journal of Materials Science and Technology, 2018, 34, 2307-2315.	10.7	28
232	Evaluation of the mechanical properties of thin metal films. Surface and Coatings Technology, 1999, 116-119, 128-132.	4.8	27
233	The structural characteristics and mechanical behaviors of nonstoichiometric apatite coatings sintered in air atmosphere. , 1999, 45, 198-203.		27
234	A Computational Study of Plastic Deformation in AISI 304 Induced by Surface Mechanical Attrition Treatment. Mechanics of Advanced Materials and Structures, 2011, 18, 572-577.	2.6	27

#	Article	IF	CITATIONS
235	Dislocation Strengthening without Ductility Trade-off in Metastable Austenitic Steels. Scientific Reports, 2016, 6, 35345.	3.3	27
236	Dissolution response of hydroxyapatite coatings to residual stresses. Journal of Biomedical Materials Research Part B, 2001, 55, 596-602.	3.1	26
237	Numerical simulation of the fluid–structure interaction for two simple fuel assemblies. Nuclear Engineering and Design, 2013, 258, 1-12.	1.7	26
238	Zirconium silicate growth induced by the thermochemical interaction of yttria-stablized zirconia coatings with molten CMAS deposits. Corrosion Science, 2019, 149, 249-256.	6.6	26
239	Characterization of the Corrosion of Nanostructured 17-4 PH Stainless Steel by Surface Mechanical Attrition Treatment (SMAT). Analytical Letters, 2019, 52, 2454-2471.	1.8	26
240	Simple Designed Micro–Nano Si–Graphite Hybrids for Lithium Storage. Small, 2021, 17, e2006373.	10.0	26
241	Insertable and reusable SERS sensors for rapid on-site quality control of fish and meat products. Chemical Engineering Journal, 2021, 426, 130733.	12.7	26
242	Metallic glasses: Gaining plasticity for microsystems. Jom, 2010, 62, 93-98.	1.9	25
243	Prestressed Fiber Bragg Grating With High Temperature Stability. Journal of Lightwave Technology, 2011, 29, 1555-1559.	4.6	25
244	Electrochemical dealloying using pulsed voltage waveforms and its application for supercapacitor electrodes. Journal of Power Sources, 2014, 257, 374-379.	7.8	25
245	Synthesis of g-C ₃ N ₄ /Silica Gels for White-Light-Emitting Devices. Particle and Particle Systems Characterization, 2017, 34, 1600258.	2.3	25
246	Bottom-up synthesis of iron and nitrogen dual-doped porous carbon nanosheets for efficient oxygen reduction. Chemical Communications, 2019, 55, 5789-5792.	4.1	25
247	Role of Boron in Enhancing Electron Delocalization to Improve Catalytic Activity of Fe-Based Metallic Glasses for Persulfate-Based Advanced Oxidation. ACS Applied Materials & Interfaces, 2020, 12, 44789-44797.	8.0	25
248	Dislocations across interphase enable plain steel with high strength-ductility. Science Bulletin, 2021, 66, 1058-1062.	9.0	25
249	APPLICATIONS OF THE INCREMENTAL HOLE-DRILLING METHOD FOR MEASUREMENT OF RESIDUAL-STRESS DISTRIBUTION. Experimental Techniques, 1989, 13, 18-24.	1.5	24
250	Numerical modeling of nanostructured materials. Finite Elements in Analysis and Design, 2010, 46, 165-180.	3.2	24
251	Design of Fe,N co-doped multi-walled carbon nanotubes for efficient oxygen reduction. Chemical Communications, 2020, 56, 14467-14470.	4.1	24
252	An inverse approach for constructing residual stress using BEM. Engineering Analysis With Boundary Elements, 2004, 28, 205-211.	3.7	23

#	Article	IF	CITATIONS
253	Nanocrystallization of zirconium subjected to surface mechanical attrition treatment. Nanotechnology, 2008, 19, 165706.	2.6	23
254	Introducing a hierarchical structure for fabrication of a high performance steel. Materials Chemistry and Physics, 2011, 129, 1096-1103.	4.0	23
255	Computer simulation of strength and ductility of nanotwin-strengthened coarse-grained metals. Modelling and Simulation in Materials Science and Engineering, 2014, 22, 075014.	2.0	23
256	Fast secondary relaxation and plasticity initiation in metallic glasses. National Science Review, 2018, 5, 616-618.	9.5	23
257	Predicting surface deformation during mechanical attrition of metallic alloys. Npj Computational Materials, 2019, 5, .	8.7	23
258	Comparison of modified injection molding and conventional machining in biodegradable behavior of perforated cannulated magnesium hip stents. Journal of Materials Science and Technology, 2021, 63, 145-160.	10.7	23
259	Multicomponent Ni-rich high-entropy alloy toughened with irregular-shaped precipitates and serrated grain boundaries. Scripta Materialia, 2021, 204, 114066.	5.2	23
260	Diffusion of Cr in Nanostructured Fe and Low Carbon Steel Produced by Means of Surface Mechanical Attrition Treatment. Defect and Diffusion Forum, 2006, 249, 147-154.	0.4	22
261	Extracting the plastic properties of metal materials from microindentation tests: Experimental comparison of recently published methods. Journal of Materials Research, 2007, 22, 1512-1519.	2.6	22
262	In situ synthesis of nanocrystalline intermetallic layer during surface plastic deformation of zirconium. Surface and Coatings Technology, 2007, 202, 583-589.	4.8	22
263	Die fatigue life improvement through the rational design of metal-forming system. Journal of Materials Processing Technology, 2009, 209, 1074-1084.	6.3	22
264	Mechanism of vertical crack formation in Yb2SiO5 coatings deposited via plasma spray-physical vapor deposition. Journal of Materiomics, 2020, 6, 102-108.	5.7	22
265	Directâ€Ink Written Shapeâ€Morphing Film with Rapid and Programmable Multimotion. Advanced Materials Technologies, 2020, 5, 1900974.	5.8	22
266	Additiveâ€Free Energetic Film Based on Graphene Oxide and Nanoscale Energetic Coordination Polymer for Transient Microchip. Advanced Functional Materials, 2021, 31, 2103199.	14.9	22
267	Examination of thermal properties by scanning thermal microscopy in ultrafine-grained pure titanium surface layer produced by surface mechanical attrition treatment. Thermochimica Acta, 2004, 419, 239-246.	2.7	21
268	Analysis of thermal properties by scanning thermal microscopy in nanocrystallized iron surface induced by ultrasonic shot peening. Materials Science & Engineering A: Structural Materials: Properties, Microstructure and Processing, 2004, 369, 36-42.	5.6	21
269	Formation of nanoporous titania on bulk titanium by hybrid surface mechanical attrition treatment. Surface and Coatings Technology, 2007, 201, 6285-6289.	4.8	21
270	Surface evolution of a gradient structured Ti in hydrogen peroxide solution. Applied Surface Science, 2008, 254, 2905-2910.	6.1	21

#	Article	IF	CITATIONS
271	Characterization of plastically graded nanostructured material: Part I. The theories and the inverse algorithm of nanoindentation. Mechanics of Materials, 2010, 42, 559-569.	3.2	21
272	A new method for the reconstruction of micro- and nanoscale planar periodic structures. Ultramicroscopy, 2010, 110, 1223-1230.	1.9	21
273	Two softening stages in nanotwinned Cu. Philosophical Magazine, 2014, 94, 4037-4052.	1.6	21
274	Numerical investigation of fracture behavior of nanostructured Cu with bimodal grain size distribution. Acta Mechanica, 2014, 225, 1093-1106.	2.1	21
275	Deformation and failure mechanisms of nanotwinned copper films with a pre-existing crack. Materials Science & Engineering A: Structural Materials: Properties, Microstructure and Processing, 2014, 606, 334-345.	5.6	21
276	Structural Signature of Plasticity Unveiled by Nano-Scale Viscoelastic Contact in a Metallic Glass. Scientific Reports, 2016, 6, 29357.	3.3	21
277	Size-dependent formation and thermal stability of high-order twins in hierarchical nanotwinned metals. International Journal of Plasticity, 2020, 128, 102685.	8.8	21
278	Revealing carbide precipitation effects and their mechanisms during quenching-partitioning-tempering of a high carbon steel: Experiments and Modeling. Acta Materialia, 2021, 217, 117176.	7.9	21
279	Investigation of the relation between structure and mechanical properties of hydrogenated diamond-like carbon coatings prepared by PECVD. Materials Science & Engineering A: Structural Materials: Properties, Microstructure and Processing, 2004, 373, 45-53.	5.6	20
280	Mesh dependence of transverse cracking in laminated metals with nanograined interface layers. Engineering Fracture Mechanics, 2013, 105, 211-220.	4.3	20
281	Hydrothermal preparation of hierarchical MoS2-reduced graphene oxide nanocomposites towards remarkable enhanced visible-light photocatalytic activity. Ceramics International, 2017, 43, 2384-2388.	4.8	20
282	Understanding the mechanical characteristics of nanotwinned diamond by atomistic simulations. Carbon, 2018, 127, 320-328.	10.3	20
283	Synergistic function of iron and cobalt in metallic glasses for highly improving persulfate activation in water treatment. Journal of Alloys and Compounds, 2020, 822, 153574.	5.5	20
284	Influence of co-existing medium Mn and dual phase steel microstructures on ductility and Lüders band formation. Acta Materialia, 2021, 221, 117418.	7.9	20
285	Four-point bending tests of thermally produced WC-Co coatings. Surface and Coatings Technology, 1996, 78, 284-294.	4.8	19
286	Characterization of the thermal properties by scanning thermal microscopy in ultrafine-grained iron surface layer produced by ultrasonic shot peening. Materials Chemistry and Physics, 2006, 96, 59-65.	4.0	19
287	Lightweight structure design for wind energy by integrating nanostructured materials. Materials & Design, 2014, 57, 689-696.	5.1	19
288	Prediction of mechanical properties in bimodal nanotwinned metals with a composite structure. Composites Science and Technology, 2016, 123, 222-231.	7.8	19

#	Article	IF	CITATIONS
289	Enhanced repeated frictional sliding properties in 304 stainless steel with a gradient nanostructured surface. Surface and Coatings Technology, 2018, 339, 14-19.	4.8	19
290	Effect of water vapor on high-temperature oxidation of NiAl alloy. Corrosion Science, 2020, 177, 108963.	6.6	19
291	Plasmonic metal nanostructures: concepts, challenges and opportunities in photo-mediated chemical transformations. IScience, 2021, 24, 101982.	4.1	19
292	Microstructural analysis by scanning thermal microscopy of a nanocrystalline Fe surface induced by ultrasonic shot peening. Superlattices and Microstructures, 2004, 35, 445-453.	3.1	18
293	Generation of Nanostructures on 316L Stainless Steel and Its Effect on Mechanical Behavior. Materials Science Forum, 2005, 490-491, 625-630.	0.3	18
294	Size effects on the ductile/brittle fracture properties of the pressure vessel steel 20g. Theoretical and Applied Fracture Mechanics, 2008, 50, 124-131.	4.7	18
295	Numerical study on the deformation behaviors of the flexible die forming by using viscoplastic pressure-carrying medium. Computational Materials Science, 2009, 46, 1058-1068.	3.0	18
296	Revelation of the effect of structural heterogeneity on microplasticity in bulk metallic-glasses. Journal of Materials Research, 2010, 25, 563-575.	2.6	18
297	Thermal Stability of Nanocrystalline AZ31 Magnesium Alloy Fabricated by Surface Mechanical Attrition Treatment. Acta Metallurgica Sinica (English Letters), 2015, 28, 1162-1169.	2.9	18
298	Super square carbon nanotube network: a new promising water desalination membrane. Npj Computational Materials, 2016, 2, .	8.7	18
299	Nanoâ€Dualâ€Phase Metallic Glass Film Enhances Strength and Ductility of a Gradient Nanograined Magnesium Alloy. Advanced Science, 2020, 7, 2001480.	11.2	18
300	Development of high-performance energy absorption component based on the structural design and nanocrystallization. Materials and Design, 2018, 137, 214-225.	7.0	18
301	Novel multilayer structure design of metallic glass film deposited Mg alloy with superior mechanical properties and corrosion resistance. Intermetallics, 2015, 62, 22-26.	3.9	17
302	Formation of a new incoherent twin boundary in a Mg–3Gd alloy. Scripta Materialia, 2016, 112, 136-139.	5.2	17
303	The Twisting of Domeâ€Like Metamaterial from Brittle to Ductile. Advanced Science, 2021, 8, 2002701.	11.2	17
304	Prediction of Residual Stress Relaxation During Fatigue. , 1988, , 75-90.		17
305	Thermal shock resistance of TiC coatings plasma sprayed onto macroroughened substrates. Surface and Coatings Technology, 1992, 53, 49-56.	4.8	16
306	Study on the reduction of tensile strength of concrete due to triaxial compressive loading history. Magazine of Concrete Research, 2002, 54, 113-124.	2.0	16

#	Article	IF	CITATIONS
307	Size-dependent sharp indentation-II: a reverse algorithm to identify plastic properties of metallic materials. Journal of the Mechanics and Physics of Solids, 2005, 53, 49-62.	4.8	16
308	Size-dependent sharp indentation?I: a closed-form expression of the indentation loading curve. Journal of the Mechanics and Physics of Solids, 2005, 53, 33-48.	4.8	16
309	Characterization of plastically graded nanostructured material: Part II. The experimental validation in surface nanostructured material. Mechanics of Materials, 2010, 42, 698-708.	3.2	16
310	Grain size gradient length scale in ballistic properties optimization of functionally graded nanocrystalline steel plates. Scripta Materialia, 2013, 69, 773-776.	5.2	16
311	The influence of interface structure on nanocrystalline deformation of a layered and nanostructured steel. Materials & Design, 2013, 47, 316-322.	5.1	16
312	Full olor Reflective Filters in a Large Area with a Wideâ€Band Tunable Absorber Deposited by Oneâ€Step Magnetron Sputtering. Advanced Optical Materials, 2020, 8, 1901626.	7.3	16
313	Fe,N Co-Doped Mesoporous Carbon Nanosheets for Oxygen Reduction. ACS Applied Nano Materials, 2020, 3, 5637-5644.	5.0	16
314	Structural engineering of sulfur-doped carbon encapsulated bismuth sulfide core-shell structure for enhanced potassium storage performance. Nano Research, 2021, 14, 3545-3551.	10.4	16
315	Selfâ€Antiâ€Stacking 2D Metal Phosphide Loopâ€Sheet Heterostructures by Edgeâ€Topological Regulation for Highly Efficient Water Oxidation. Small, 2021, 17, e2006860.	10.0	16
316	Study of Surface Residual Stress by Three-Dimensional Displacement Data at a Single Point in Hole Drilling Method. Journal of Engineering Materials and Technology, Transactions of the ASME, 2000, 122, 215-220.	1.4	15
317	Surface Nanocrystallization (SNC) of Materials and its Effect on Mechanical Behavior. , 2003, , 495-528.		15
318	Nano-scratch experiments of Au/NiCr multi-layered films for microwave integrated circuits. Surface and Coatings Technology, 2007, 201, 5664-5666.	4.8	15
319	Surface mechanical attrition treatment induced phase transformation behavior in NiTi shape memory alloy. Journal of Alloys and Compounds, 2009, 482, 298-301.	5.5	15
320	Thermal stability and corrosion resistance of nanocrystallized zirconium formed by surface mechanical attrition treatment. Journal of Materials Research, 2009, 24, 3136-3145.	2.6	15
321	FE Simulation-Based Folding Defect Prediction and Avoidance in Forging of Axially Symmetrical Flanged Components. Journal of Manufacturing Science and Engineering, Transactions of the ASME, 2010, 132, .	2.2	15
322	Superplasticity deformation of Ti–6Al–2Zr–1Mo–1V induced by the cyclic change of strain-rate and MaxmSPD. Journal of Alloys and Compounds, 2010, 491, 213-217.	5.5	15
323	Measurement of interfacial toughness of metal film wire and polymer membrane through electricity induced buckling method. Journal of Colloid and Interface Science, 2011, 358, 491-496.	9.4	15
324	Study on wear and friction resistance of nanocrystalline Fe nitrided at low temperature. Wear, 2011, 271, 653-657.	3.1	15

#	Article	IF	CITATIONS
325	Preventing debonding at the steel to concrete interface through strain localization. Composites Part B: Engineering, 2013, 45, 1061-1070.	12.0	15
326	Effect of warm deformation on microstructure and mechanical properties of a layered and nanostructured 304 stainless steel. Materials Science & Engineering A: Structural Materials: Properties, Microstructure and Processing, 2014, 595, 34-42.	5.6	15
327	An extremely superhydrophobic and intrinsically stable Si/fluorocarbon energetic composite based on upright nano/submicron-sized Si wire arrays. RSC Advances, 2015, 5, 106098-106106.	3.6	15
328	Atomistic simulation study on twin orientation and spacing distribution effects on nanotwinned Cu films. Philosophical Magazine, 2015, 95, 3467-3485.	1.6	15
329	Synthesis of fluorine-doped <i>α</i> -Fe ₂ O ₃ nanorods toward enhanced lithium storage capability. Nanotechnology, 2017, 28, 065401.	2.6	15
330	A robust spring-like lamellar VO/C nanostructure for high-rate and long-life potassium-ion batteries. Journal of Materials Chemistry A, 2020, 8, 23939-23946.	10.3	15
331	Microstructure Evolution and Mechanical Properties of Austenite Stainless Steel with Gradient Twinned Structure by Surface Mechanical Attrition Treatment. Nanomaterials, 2021, 11, 1624.	4.1	15
332	Second phase effect on corrosion of nanostructured Mg-Zn-Ca dual-phase metallic glasses. Journal of Magnesium and Alloys, 2021, 9, 1546-1555.	11.9	15
333	A systematic study of the validation of Oliver and Pharr's method. Journal of Materials Research, 2007, 22, 3385-3396.	2.6	14
334	Deformation-induced ambient temperature α-to-β phase transition and nanocrystallization in (α + β) titanium alloy. Journal of Materials Research, 2009, 24, 3439-3445.	2.6	14
335	High Strength Nanocrystallized Multilayered Structure Obtained by SMAT and Co-Rolling. Materials Science Forum, 2009, 614, 249-254.	0.3	14
336	Improved plasticity and fracture toughness in metallic glasses via surface crystallization. Intermetallics, 2011, 19, 1420-1427.	3.9	14
337	Resonance ultrasonic actuation and local structural rejuvenation in metallic glasses. Physical Review B, 2017, 95, .	3.2	14
338	Bistable metallic materials produced by nanocrystallization process. Materials and Design, 2018, 141, 374-383.	7.0	14
339	<i>>g</i> ₃ N ₄ â€Modified Waterâ€Crystallized Mesoporous SnO ₂ for Enhanced Photoelectrochemical Properties. Particle and Particle Systems Characterization, 2018, 35, 1800155.	2.3	14
340	Controlling Plasmon-Aided Reduction of <i>p</i> -Nitrothiophenol by Tuning the Illumination Wavelength. ACS Catalysis, 2021, 11, 14898-14905.	11.2	14
341	An anti-freezing biomineral hydrogel of high strain sensitivity for artificial skin applications. Nano Research, 2022, 15, 6655-6661.	10.4	14
342	Mineral Hydrogel from Inorganic Salts: Biocompatible Synthesis, Allâ€inâ€One Charge Storage, and Possible Implications in the Origin of Life. Advanced Functional Materials, 2022, 32, .	14.9	14

#	Article	IF	CITATIONS
343	Insertable, Scabbarded, and Nanoetched Silver Needle Sensor for Hazardous Element Depth Profiling by Laser-Induced Breakdown Spectroscopy. ACS Sensors, 2022, 7, 1381-1389.	7.8	14
344	The nano-scratch behaviour of different diamond-like carbon film–substrate systems. Journal Physics D: Applied Physics, 2004, 37, 2135-2139.	2.8	13
345	FEA-aided design of multi-stage drawing process and tooling for production of a miniature sheet metal component. International Journal of Advanced Manufacturing Technology, 2010, 46, 993-1000.	3.0	13
346	The elastic T-stress for slightly curved or kinked cracks. International Journal of Solids and Structures, 2010, 47, 1753-1763.	2.7	13
347	Study of toughening mechanisms through the observations of crack propagation in nanostructured and layered metallic sheet. Materials Science & Engineering A: Structural Materials: Properties, Microstructure and Processing, 2011, 528, 8389-8395.	5.6	13
348	A study of dynamic plasticity in austenite stainless steels with a gradient distribution of nanoscale twins. Scripta Materialia, 2017, 133, 49-53.	5.2	13
349	Nanostructured laminar tungsten alloy with improved ductility by surface mechanical attrition treatment. Scientific Reports, 2017, 7, 1351.	3.3	13
350	Tunable Transformation Between SnS and SnO _x Nanostructures via Facile Anodization and Their Photoelectrochemical and Photocatalytic Performance. Solar Rrl, 2018, 2, 1800161.	5.8	13
351	Mechanical behaviour of AZ31 magnesium alloy with the laminate and gradient structure. Philosophical Magazine, 2019, 99, 3059-3077.	1.6	13
352	The combined effects of grain and sample sizes on the mechanical properties and fracture modes of gold microwires. Journal of Materials Science and Technology, 2019, 35, 76-83.	10.7	13
353	Ductility of an ultrastrong glass-crystal nano-dual-phase alloy in sub-micron. Scripta Materialia, 2020, 183, 17-21.	5.2	13
354	Ferroic alternation in methylammonium lead triiodide perovskite. EcoMat, 2021, 3, e12131.	11.9	13
355	Nano-scratching process and fracture mechanism of amorphous carbon films. Wear, 2003, 254, 1032-1036.	3.1	12
356	On the determination of reduced Young's modulus and hardness of elastoplastic materials using a single sharp indenter. Journal of Materials Research, 2006, 21, 215-224.	2.6	12
357	X-ray diffraction measurement of residual stress and crystal orientation in Au/NiCr/Ta films prepared by plating. Surface and Coatings Technology, 2007, 201, 5944-5947.	4.8	12
358	Necking propagated deformation behavior of layer-structured steel prepared by co-warm rolled surface nanocrystallized 304 stainless steel. Materials Letters, 2007, 61, 5191-5193.	2.6	12
359	A new way to synthesize carbon nanofiber film on bulk titanium via hybrid surface mechanical attrition treatment. Applied Surface Science, 2013, 264, 191-196.	6.1	12
360	Nanocrystalline-grained tungsten prepared by surface mechanical attrition treatment: Microstructure and mechanical properties. Journal of Nuclear Materials, 2016, 480, 281-288.	2.7	12

#	Article	IF	CITATIONS
361	Bestow metal foams with nanostructured surfaces via a convenient electrochemical method for improved device performance. Nano Research, 2016, 9, 2364-2371.	10.4	12
362	Solution-Based Comproportionation Reaction for Facile Synthesis of Black TiO ₂ Nanotubes and Nanoparticles. ACS Applied Energy Materials, 2020, 3, 6087-6092.	5.1	12
363	Récents développements de la mesure des contraintes résiduelles par perçage incrémental. Materiaux Et Techniques, 1985, 73, 709-718.	0.9	12
364	Self-templated formation of twin-like metal-organic framework nanobricks as pre-catalysts for efficient water oxidation. Nano Research, 2022, 15, 2887-2894.	10.4	12
365	Residual stresses in plasma-sprayed hydroxyapatite coatings. Journal of Materials Science Letters, 1999, 18, 1087-1089.	0.5	11
366	Determination of Residual Stress in Z8CDWV12 Steel Using Critically Refracted Longitudinal Waves JSME International Journal Series A-Solid Mechanics and Material Engineering, 2000, 43, 367-373.	0.4	11
367	Study of Nonuniform In-Plane and In-Depth Residual Stress of Friction Stir Welding. Journal of Pressure Vessel Technology, Transactions of the ASME, 2003, 125, 201-208.	0.6	11
368	An inverse approach to construct residual stresses existing in axisymmetric structures using BEM. Engineering Analysis With Boundary Elements, 2005, 29, 986-999.	3.7	11
369	Deformation and crystallization of a Zr41.2Ti13.8Cu12.5Ni10Be22.5 bulk metallic glass in the supercooled liquid region. Materials Science & Engineering A: Structural Materials: Properties, Microstructure and Processing, 2006, 435-436, 405-411.	5.6	11
370	Nanocrystalline Titanium to Mesoporous Anatase with High Bioactivity. Crystal Growth and Design, 2007, 7, 2400-2403.	3.0	11
371	Can Young's modulus and hardness of wire structural materials be directly measured using nanoindentation?. Journal of Materials Research, 2009, 24, 1054-1058.	2.6	11
372	Smart polymers for textile applications. , 2014, , 437-475.		11
373	Bulk monolithic electrodes enabled by surface mechanical attrition treatment-facilitated dealloying. Journal of Materials Chemistry A, 2016, 4, 15057-15063.	10.3	11
374	Strain rate dependent hyperelastic stress-stretch behavior of a silica nanoparticle reinforced poly (ethylene glycol) diacrylate nanocomposite hydrogel. Journal of the Mechanical Behavior of Biomedical Materials, 2017, 75, 236-243.	3.1	11
375	Light-weight isometric-phase steels with superior strength-hardness-ductility combination. Scripta Materialia, 2018, 154, 230-235.	5.2	11
376	Deformation mechanism and dynamic precipitation in a Mg-7Al-2Sn alloy processed by surface mechanical attrition treatment. Journal of Materials Science and Technology, 2019, 35, 1473-1478.	10.7	11
377	Medical Additive Manufacturing: From a Frontier Technology to the Research and Development of Products. Engineering, 2020, 6, 1217-1221.	6.7	11
378	Continuous morphing trailing-edge wing concept based on multi-stable nanomaterial. Chinese Journal of Aeronautics, 2021, 34, 219-231.	5.3	11

#	Article	IF	CITATIONS
379	Soft, Bistable Actuators for Reconfigurable 3D Electronics. ACS Applied Materials & Interfaces, 2021, 13, 41968-41977.	8.0	11
380	Thermal-induced inverse γ/α′ phase transformation in surface nanocrystallization layer of 304 stainless steel. Surface and Coatings Technology, 2007, 201, 7462-7466.	4.8	10
381	Efficient Ternary CdSSe Quantumâ€Dotâ€6ensitized Solar Cells based on MgOâ€coated TiO ₂ Nanoparticles. Energy Technology, 2014, 2, 526-530.	3.8	10
382	Serrated plastic flow behavior and microstructure in a Zr-based bulk metallic glass processed by surface mechanical attrition treatment. Journal of Iron and Steel Research International, 2017, 24, 475-482.	2.8	10
383	Atomic scale study of the anti-vortex domain structure in polycrystalline ferroelectric. Philosophical Magazine, 2018, 98, 118-138.	1.6	10
384	Near-ideal strength and large compressive deformability of a nano-dual-phase glass-crystal alloy in sub-micron. Scripta Materialia, 2020, 188, 290-295.	5.2	10
385	Constitutive modeling of size-dependent deformation behavior in nano-dual-phase glass-crystal alloys. International Journal of Plasticity, 2021, 137, 102918.	8.8	10
386	Modelling of the Ultrasonic Shot Peening Process. Materials Science Forum, 2005, 490-491, 67-72.	0.3	9
387	Isothermal internal friction behaviour of a Zr based bulk metallic glass with large supercooled liquid region. Journal Physics D: Applied Physics, 2006, 39, 2851-2855.	2.8	9
388	Dual character of stable shear banding in bulk metallic glasses. Intermetallics, 2011, 19, 1005-1013.	3.9	9
389	Surface Hardening of NiTi Shape Memory Alloy Induced by the NanoStructured Layer After Surface Mechanical Attrition Treatment. Journal of Nanoscience and Nanotechnology, 2011, 11, 10954-10957.	0.9	9
390	Electrochemical fabrication and optical properties of porous tin oxide films with structural colors. Journal of Applied Physics, 2014, 116, .	2.5	9
391	Surface-modified steel sheets and corrugated panels in three-point bending. International Journal of Mechanical Sciences, 2018, 142-143, 10-20.	6.7	9
392	Various configurations and transition strategies of nanostructure induced bistable disks. International Journal of Solids and Structures, 2019, 160, 80-95.	2.7	9
393	Biaxial fatigue crack growth in proton exchange membrane of fuel cells based on cyclic cohesive finite element method. International Journal of Mechanical Sciences, 2021, 189, 105946.	6.7	9
394	Experimental Study of Residual Stress Distributions in Quenched Parts by the Incremental Large Hole Drilling Method and by the Neutron Diffraction Method. Journal of Testing and Evaluation, 2000, 28, 282-289.	0.7	9
395	Local thermal property analysis by scanning thermal microscopy of an ultrafine-grained copper surface layer produced by surface mechanical attrition treatment. Materials Science and Engineering B: Solid-State Materials for Advanced Technology, 2006, 130, 24-30.	3.5	8
396	Dependence of the representative strain on the hardening functions of metallic materials in indentation. Scripta Materialia, 2007, 57, 57-60.	5.2	8

#	Article	IF	CITATIONS
397	Microstructure promoted photosensitization activity of dye-titania/titanium composites. Composites Part A: Applied Science and Manufacturing, 2008, 39, 690-696.	7.6	8
398	Numerical Simulation of Multiple Cracking in ANSI 304 Stainless Steel Under Thermal Fatigue. International Journal of Damage Mechanics, 2010, 19, 767-785.	4.2	8
399	Electrochemical Fabrication of Coaxial Wavyâ€Channel Ni ^{III} O(OH)/Ni Nanocomposites for Highâ€Performance Supercapacitor Electrode Materials. Energy Technology, 2013, 1, 478-483.	3.8	8
400	Stress induced atomic-scale damage and relaxation in bulk metallic glasses. Journal of Alloys and Compounds, 2015, 652, 185-190.	5.5	8
401	Precipitation behavior of bulk nanocrystalline GW103K alloy induced by surface mechanical attrition treatment. Journal of Alloys and Compounds, 2017, 697, 282-286.	5.5	8
402	Interface effects on the strength and ductility of bimodal nanostructured metals. Acta Mechanica, 2018, 229, 3475-3487.	2.1	8
403	Mechanical properties and corrosion behaviors of AZ31 alloy with dual-phase glass-crystal coating. Materials Characterization, 2019, 154, 200-211.	4.4	8
404	Low-carbon advanced nanostructured steels: Microstructure, mechanical properties, and applications. Science China Materials, 2021, 64, 1580-1597.	6.3	8
405	Supervariate ceramics: biomineralization mechanism. Materials Today Advances, 2021, 10, 100144.	5.2	8
406	Interfacial oxidation of hafnium modified NiAl alloys. Corrosion Science, 2021, 189, 109604.	6.6	8
407	Waterâ€assisted sintering of silica: Densification mechanisms and their possible implications in biomineralization. Journal of the American Ceramic Society, 2022, 105, 2945-2954.	3.8	8
408	Tunable ultrathin dual-phase P-doped Bi2MoO6 nanosheets for advanced lithium and sodium storage. Nano Research, 2022, 15, 6128-6137.	10.4	8
409	Study of Cr2O3 coatings Part II: Adhesion to a cast-iron substrate. Journal of Thermal Spray Technology, 1995, 4, 347-352.	3.1	7
410	Estimation of residual stresses induced by shot-peening. Measurement of the thermal dissipation with an infrared camera. International Journal of Thermal Sciences, 2002, 41, 369-375.	4.9	7
411	Influence of residual stresses on the mechanical behavior of composite laminate materials. Advanced Composite Materials, 2005, 14, 319-342.	1.9	7
412	Experimental and Theoretical Investigation of Size Effects on the Ductile/Brittle Fracture Toughness of a Pressure Steel. International Journal of Damage Mechanics, 2010, 19, 611-629.	4.2	7
413	Control of iron nitride formation by a high magnetic field. Journal of Materials Research, 2010, 25, 2082-2085.	2.6	7
414	Tensile deformation properties of single crystal copper with nanotwins. Computational Materials Science, 2014, 83, 269-276.	3.0	7

#	Article	IF	CITATIONS
415	Efficiency improvement in silicon nanowire/conductive polymer hybrid solar cells based on formic acid treatment. RSC Advances, 2016, 6, 86836-86842.	3.6	7
416	Investigation on snapping transitions of locally nanostructured bistable disks actuated by distributed transverse forces. Mechanics of Materials, 2018, 127, 91-99.	3.2	7
417	Brittle-to-ductile transition of Au2Al and AuAl2 intermetallic compounds in wire bonding. Journal of Materials Science: Materials in Electronics, 2019, 30, 862-866.	2.2	7
418	Cellular fate of deformable needle-shaped PLGA-PEG fibers. Acta Biomaterialia, 2020, 112, 182-189.	8.3	7
419	Anodic self-assembly method for synthesizing hierarchical FeS/FeOx hollow nanospheres. Journal of Power Sources, 2021, 484, 229268.	7.8	7
420	Supervariate Ceramics: Gelatinous and Monolithic Ceramics Fabricated under Ambient Conditions. Advanced Engineering Materials, 0, , 2100866.	3.5	7
421	Sphere Packing and Applications to Granular Structure Modeling. , 2008, , 1-18.		7
422	Simulation on bone remodeling with stochastic nature of adult and elderly using topology optimization algorithm. Journal of Biomechanics, 2022, 136, 111078.	2.1	7
423	Encapsulating atomic molybdenum into hierarchical nitrogen-doped carbon nanoboxes for efficient oxygen reduction. Journal of Colloid and Interface Science, 2022, 620, 67-76.	9.4	7
424	A Study of Process-Induced Residual Stress in PBGA Packages. Journal of Electronic Packaging, Transactions of the ASME, 2000, 122, 262-266.	1.8	6
425	Round Robin Test on the Determination of Residual Stress Depth Distributions by X-ray Diffraction. Materials Science Forum, 2002, 404-407, 659-664.	0.3	6
426	Mechanics of High Strength and High Ductility Materials. Procedia Engineering, 2011, 10, 2202-2207.	1.2	6
427	Reinforcement of laser-welded stainless steels by surface mechanical attrition treatment. Materials Science & Engineering A: Structural Materials: Properties, Microstructure and Processing, 2013, 571, 161-166.	5.6	6
428	Wide angle and narrow-band asymmetric absorption in visible and near-infrared regime through lossy Bragg stacks. Scientific Reports, 2016, 6, 27061.	3.3	6
429	Microstructureâ€Property Relations in the Tensile Behavior of Bimodal Nanostructured Metals. Advanced Engineering Materials, 2020, 22, 2000097.	3.5	6
430	A constitutive model incorporating grain refinement strengthening on metallic alloys. Journal of Materials Science and Technology, 2021, 88, 233-239.	10.7	6
431	Determining Residual Stress in Spherical Components: A New Application of the Hole-Drilling Method. Journal of Testing and Evaluation, 2004, 32, 11627.	0.7	6
432	Water Splitting: A Novel Multinary Intermetallic as an Active Electrocatalyst for Hydrogen Evolution (Adv. Mater. 21/2020). Advanced Materials, 2020, 32, 2070166.	21.0	6

#	Article	IF	CITATIONS
433	Design Tool on Fatigue for 3D Components With Consideration of Residual Stresses. , 2001, , .		5
434	Ultrasonic Evaluation of Compressive Residual Stress of Surface Treated Metals. Materials Science Forum, 2005, 490-491, 184-189.	0.3	5
435	Effects of sample geometry on deformation modes of bulk metallic glasses at the nano/micrometer scale. Journal of Materials Research, 2009, 24, 3465-3468.	2.6	5
436	Development of a Micro-beam Method to Investigate the Fatigue Crack Growth Mechanisms of Submicron-scale Cracks. Experimental Mechanics, 2009, 49, 731-742.	2.0	5
437	FEM-Based Modeling of Dynamic Recrystallization of AISI 52100 Steel Using Cellular Automaton Method. Key Engineering Materials, 0, 447-448, 406-411.	0.4	5
438	Application of Moiré Interferometry to Study Residual Deformation in Lapâ€Welded Steel Plates. Strain, 2011, 47, 311-319.	2.4	5
439	Surface Stress Effects on the Yield Strength in Nanotwinned Polycrystal Face-Centered-Cubic Metallic Nanowires. Journal of Applied Mechanics, Transactions ASME, 2014, 81, .	2.2	5
440	Lead-induced stress corrosion cracking behavior of mechanically surface-treated alloy 690. Materials Research Letters, 2016, 4, 180-184.	8.7	5
441	Improving bistable properties of metallic shells using a nanostructuring technique. Thin-Walled Structures, 2020, 146, 106444.	5.3	5
442	Facile Surfactantâ€; Reductantâ€; and Ag Saltâ€free Growth of Ag Nanoparticles with Controllable Size from 35 to 660 nm on Bulk Ag Materials. Chemistry - an Asian Journal, 2021, 16, 2249-2252.	3.3	5
443	In situ surface-enhanced Raman spectroscopy monitoring of molecular reorientation in plasmon-mediated chemical reactions. Journal of Catalysis, 2022, 413, 527-533.	6.2	5
444	A highly accurate brick element based on a three-field variational principle for elasto-plastic analysis. Finite Elements in Analysis and Design, 2003, 39, 1155-1171.	3.2	4
445	Determination of the Residual Stresses in Composite Laminate Using the Compliance Method. Materials Science Forum, 2005, 490-491, 533-538.	0.3	4
446	An Advanced Residual Stress Determination for 3D Cylinder Structure. Materials Science Forum, 2005, 490-491, 62-66.	0.3	4
447	Use of Full Field of Strains Found By Grating Shearography to Determine Residual Stress. Journal of Strain Analysis for Engineering Design, 2005, 40, 621-630.	1.8	4
448	Effect of Surface Nano Crystallization on Tribological Properties of Stainless Steel. Materials Science Forum, 2006, 524-525, 717-722.	0.3	4
449	Thermal-stress analysis for a strip of finite width containing a stack of edge cracks. Journal of Engineering Mathematics, 2008, 61, 161-169.	1.2	4
450	A fast and accurate analysis of the interacting cracks in linear elastic solids. International Journal of Fracture, 2008, 151, 169-185.	2.2	4

#	Article	IF	CITATIONS
451	Modélisation géométrique des structures granulaires. Comptes Rendus - Mecanique, 2008, 336, 506-511.	2.1	4
452	Tensile Properties of Different Silkworm Silk Fibers. Advanced Materials Research, 0, 47-50, 1213-1216.	0.3	4
453	Proximity gettering of Cu at a (110)/(001) grain boundary interface formed by direct silicon bonding. Applied Physics Letters, 2009, 94, 221909.	3.3	4
454	Influence of hardening behaviour of elastoplastic materials on the determination of elastic modulus using indentation tests. Materials Science & Engineering A: Structural Materials: Properties, Microstructure and Processing, 2010, 527, 4571-4575.	5.6	4
455	Ultrasound driven aggregation—A novel method to assemble ceramic nanoparticles. Extreme Mechanics Letters, 2016, 7, 71-77.	4.1	4
456	Effects of Pd Surface Coating on the Strength and Fracture Behavior of Cu Micro Bonding Wires. Metallurgical and Materials Transactions A: Physical Metallurgy and Materials Science, 2019, 50, 3013-3018.	2.2	4
457	Electrochemically Synthesized Porous Ag Double Layers for Surface-Enhanced Raman Spectroscopy Applications. Langmuir, 2019, 35, 6340-6345.	3.5	4
458	Ultrafine Nanoporous Gold <i>via</i> Thiol Compound-Mediated Chemical Dealloying. Journal of Physical Chemistry C, 2020, 124, 10026-10031.	3.1	4
459	Thermal and Nonthermal Effects in Plasmonâ€Mediated Electrochemistry at Nanostructured Ag Electrodes. Angewandte Chemie, 2020, 132, 6856-6859.	2.0	4
460	Nacre-liked material with tough and post-tunable mechanical properties. Journal of Materials Science and Technology, 2022, 114, 172-179.	10.7	4
461	Universality of quenching-partitioning-tempering local equilibrium model. Journal of Materials Science and Technology, 2022, 124, 116-120.	10.7	4
462	High sensitivity moir $ ilde{A}$ © interferometry and incremental hole-drilling method for residual stress measurement. Comptes Rendus Mecanique, 2001, 329, 585-593.	0.2	3
463	Improvement of the Fatigue Behaviour of an Automotive Part Using a New Mechanical Treatment. Materials Science Forum, 2002, 404-407, 463-468.	0.3	3
464	Determination of Compressive Residual Stresses Using Critically Refracted Longitudinal (Lcr) Waves. , 2004, , 137.		3
465	Calculation of Relaxation of Residual Stress and Change of Yield Strength in Shot Peened Layer. Materials Science Forum, 2005, 490-491, 396-403.	0.3	3
466	An updated continuum damage model to investigate fracture process of structures in DBTT region. International Journal of Fracture, 2008, 151, 199-215.	2.2	3
467	Ultrasonic Surface Mechanical Attrition of Commercially Pure Ti to Induce Nanocrystalline Surface Layer. Key Engineering Materials, 2010, 442, 152-157.	0.4	3
468	Achieving high strength and high ductility in nanostructured metals: Experiment and modelling. Theoretical and Applied Mechanics Letters, 2012, 2, 021001.	2.8	3

#	Article	IF	CITATIONS
469	Micromechanical Simulation of Fracture Behavior of Nanostructured Metals with Bimodal Grain Size Distribution. , 2014, 3, 2148-2153.		3
470	Microstructural effects of chemical island templating in patterned matrix-pillar oxide nanocomposites. CrystEngComm, 2015, 17, 2041-2049.	2.6	3
471	Effect of EFO parameters on the HAZ and bondability of gold wire. , 2018, , .		3
472	Experimental and Theoretical Investigation on Bistable Symmetric Shells Built by Locally Nanostructuring Isotropic Rectangular Plates. International Journal of Structural Stability and Dynamics, 2019, 19, 1950141.	2.4	3
473	Liquefaction-induced plasticity from entropy-boosted amorphous ceramics. Applied Materials Today, 2021, 23, 101011.	4.3	3
474	Amorphous Highâ€Entropy Hydroxides of Tunable Wide Solar Absorption for Solar Water Evaporation. Particle and Particle Systems Characterization, 2021, 38, 2100094.	2.3	3
475	Functionalized nanoporous gold membrane for pancreatic islet cells encapsulation. Materials Letters, 2021, 301, 130224.	2.6	3
476	The physical origin of observed repulsive forces between general dislocations and twin boundaries in FCC metals: An atom-continuum coupling study. Journal of Materials Science and Technology, 2022, 109, 221-227.	10.7	3
477	Emerging Intelligent Manufacturing of Metal Halide Perovskites. Advanced Materials Technologies, 2023, 8, .	5.8	3
478	Study of Residual Stress Distribution by the Combination of three Techniques in an Aluminium Based MMC. Materials Science Forum, 2000, 347-349, 498-503.	0.3	2
479	Fabrication and Nanostructured Surface Layers of Al Alloy by Surface Vibrational Mechanical Attrition. Materials Research Society Symposia Proceedings, 2001, 697, 8141.	0.1	2
480	Study of Residual Stresses in Complex Parts by Experimental and Numerical Methods. Materials Science Forum, 2002, 404-407, 251-256.	0.3	2
481	Study of the Mechanical Properties of Nanostructured Aluminum Obtained by SMAT. , 2007, , 39.		2
482	Preparation and Electrochemical Capacitance of Ruthenium Oxide-Titania Nanotube Composite. Materials Science Forum, 2009, 614, 235-241.	0.3	2
483	Microstructure Evolution and Tensile Properties of 304L Stainless Steel Subjected to Surface Mechanical Attrition Treatment. Materials Science Forum, 2010, 667-669, 175-179.	0.3	2
484	Fiber metallic glass laminates. Journal of Materials Research, 2010, 25, 2287-2291.	2.6	2
485	Residual strain evaluation of curved surface by grating-transferring technique and GPA. Theoretical and Applied Mechanics Letters, 2011, 1, 051007.	2.8	2
486	Study on Mechanical Properties of 2024 Al Sheet Treated by SMAT. Advanced Materials Research, 0, 410, 257-262.	0.3	2

#	Article	IF	CITATIONS
487	Structure, hydrophilicity and corrosion resistance of sol–gel derived Ag-containing TiO2 film on plasma nitrided 316L stainless steel. Journal of Sol-Gel Science and Technology, 2014, 69, 85-92.	2.4	2
488	A Computational Method of Residual Stress Calculation for Incremental Hole-Drilling Method Utilized Composite Materials. Materials Science Forum, 0, 813, 94-101.	0.3	2
489	Transitions of nanostructure-induced bistable disks actuated by line forces. International Journal of Mechanical Sciences, 2019, 157-158, 542-551.	6.7	2
490	A New Inner Surface Attrition Treatment for Strengthening Metallic Tubular Structures. Advanced Engineering Materials, 2019, 21, 1801125.	3.5	2
491	Luminescence in external dopant-free scandium-phosphorus vanadate solid solution: a spectroscopic and theoretical investigation. Materials Advances, 2020, 1, 2467-2482.	5.4	2
492	Microscopic Volta potential difference on metallic surface promotes the osteogenic differentiation and proliferation of human mesenchymal stem cells. Materials Science and Engineering C, 2021, 128, 112325.	7.3	2
493	MEASUREMENT OF RESIDUAL STRESS DISTRIBUTION BY THE INCREMENTAL HOLE-DRILLING METHOD. , 1987, , 199-219.		2
494	Study of the Residual Stress in Cold-Rolled 7075 Al-SiC Whisker-Reinforced Composites by X-Ray and Neutron Diffraction. Journal of Composites Technology and Research, 1995, 17, 194.	0.4	2
495	An Advanced Residual Stress Determination for 3D Cylinder Structure. Materials Science Forum, 0, , 62-66.	0.3	2
496	Diffusion of Cr in Nanostructured Fe and Low Carbon Steel Produced by Means of Surface Mechanical Attrition Treatment. Defect and Diffusion Forum, 0, , 147-154.	0.4	2
497	Tuning the strength-ductility synergy of nanograined Cu through nanotwin volume fraction. Computational Materials Science, 2022, 203, 111073.	3.0	2
498	Light-controlled multifunctional reconfigurable structures. Applied Materials Today, 2022, 26, 101393.	4.3	2
499	Supervariate Ceramics: Gelatinous and Monolithic Ceramics Fabricated under Ambient Conditions. Advanced Engineering Materials, 2021, 23, .	3.5	2
500	Influence of cold rolling and fatigue on the residual stress state of a metal matrix composite. European Physical Journal Special Topics, 1993, 03, C7-1817-C7-1820.	0.2	1
501	MECHANICAL FRINGE SHIFTING IN MOIRE INTERFEROMETRY. Experimental Techniques, 1999, 23, 16-19.	1.5	1
502	Incremental hole drilling and X-ray diffraction techniques to the residual stresses determination introduced by shot peening in titanium alloy. Journal of Neutron Research, 2001, 9, 337-344.	1.1	1
503	Generation of Extremely High Stress Levels in a TiAl Based Alloy. Materials Science Forum, 2002, 404-407, 89-94.	0.3	1
504	<title>Residual stresses of surface nanocrystalline material by moire interferometry and</td><td></td><td>1</td></tr></tbody></table></title>		

hole-drilling method</title>., 2002, ...

#	Article	IF	CITATIONS
505	A new scheme for designing the penalty factor in 3-D penalty-equilibrating mixed elements. Communications in Numerical Methods in Engineering, 2004, 20, 455-464.	1.3	1
506	Presentation of a General Approach for Taking into Account the Residual Stress in the Design of Automotive Components. , 2005, , .		1
507	Uncertainty evaluation of strain and strain rate measurements by ESPI during a tensile test. , 2006, 6341, 552.		1
508	Dependence Between Aging Treatments and Residual Stresses on Composite Laminate. Materials Science Forum, 2006, 524-525, 813-817.	0.3	1
509	Crystal Orientation and Hardness of Au/NiCr/Ta Films on Si-(111) Substrate Prepared by Magnetron Sputtering. Advanced Materials Research, 2009, 79-82, 719-722.	0.3	1
510	A SIMPLE HETERODYNE TEMPORAL SPECKLE-PATTERN INTERFEROMETER. , 2010, , .		1
511	The mechanical properties and resistivity of Au/NiCr/Ta multi-layered films on Si-(111) substrate. Thin Solid Films, 2011, 520, 824-827.	1.8	1
512	Residual stresses measurement with hole-drilling method on 6,061 aluminum under SMAT treatment. World Journal of Engineering, 2012, 9, 487-492.	1.6	1
513	Deformation twins induced by multi-mode deformation in nanocrystalline copper. Philosophical Magazine Letters, 2013, 93, 490-497.	1.2	1
514	Experimental Study on a Graded Stainless Steel Sheet under Quasi-Static and Dynamic Loading. Key Engineering Materials, 0, 535-536, 56-59.	0.4	1
515	Nanostructures: High-Strength and High-Ductility Nanostructured and Amorphous Metallic Materials (Adv. Mater. 31/2014). Advanced Materials, 2014, 26, 5517-5517.	21.0	1
516	Lattice Structures Made From Surface-Modified Steel Sheets. Journal of Applied Mechanics, Transactions ASME, 2015, 82, .	2.2	1
517	Metallic Glasses: Compelling Rejuvenated Catalytic Performance in Metallic Glasses (Adv. Mater.) Tj ETQq1 1 0.78	4314 rgB1 21.0	[Overlock]
518	Ductile Au4Al intermetallic compound with crack resistance. Intermetallics, 2019, 112, 106555.	3.9	1
519	Grain-size insensitive work-hardening behavior of Ag microwires. Materials Science & Engineering A: Structural Materials: Properties, Microstructure and Processing, 2019, 759, 655-660.	5.6	1
520	Metallic Glass Catalysts: Attractive In Situ Selfâ€Reconstructed Hierarchical Gradient Structure of Metallic Glass for High Efficiency and Remarkable Stability in Catalytic Performance (Adv. Funct.) Tj ETQq0 0 0 rgE	3T1/Øyerloo	cka 10 Tf 50 3
521	Multistable shells with designable configurations based on localized nanocrystallization processes. Materials and Design, 2020, 195, 109047.	7.0	1
522	Characterization and stability of hydroxyapatite coatings prepared by an electrodeposition and	3.1	1

#	Article	IF	CITATIONS
523	Global Mechanical Behavior of a Nanostructured Multilayered Composite Material Produced by Smat and Co-Rolling. , 2007, , 45-46.		1
524	Effect of Very High Stress Levels on the Fatigue Life of a TiAl Based Alloy. Materials Science Forum, 0, , 418-423.	0.3	1
525	Effect of Loading Schemes on Depth-Sensing Indentation Tests. Journal of Testing and Evaluation, 2004, 32, 11967.	0.7	1
526	Simulation of fluid-structure interaction for an elastic cylinder in an axial flow. , 2012, , .		1
527	Residual Stress Measurement on Coatings and Multilayer Materials Using the Step-by-Step Hole-Drilling Method. , 1989, , 103-109.		0
528	Influence of the residual stresses on the mechanical behavior of advanced composite parts. Journal of Neutron Research, 2001, 9, 319-330.	1.1	0
529	<title>Wavelet transform based on digital speckle correlation method: principle and algorithm</title> . , 2002, 4537, 402.		0
530	Study of Residual Stresses in Composite Laminates by the Finite Element Method and Experimental Analysis. Materials Science Forum, 2002, 404-407, 925-0.	0.3	0
531	Moire interferometry and hole drilling system for residual stress measurement. , 2003, , .		0
532	OS06W0380 Recent developments of surface nanocristalization of metallic material. The Abstracts of ATEM International Conference on Advanced Technology in Experimental Mechanics Asian Conference on Experimental Mechanics, 2003, 2003.2, _OS06W0380OS06W0380.	0.0	0
533	Effect of Very High Stress Levels on the Fatigue Life of a TiAl Based Alloy. Materials Science Forum, 2005, 490-491, 418-423.	0.3	0
534	Ultrasonic Measurement of Residual Stress in SMAT Metals. , 2006, , .		0
535	Residual Stress Analysis in Crankshaft Using the Hole Drilling Method. Materials Science Forum, 2006, 524-525, 537-542.	0.3	0
536	Surface Morphology, Crystal Orientation and Scratch Properties of Au/NiCr/Ta Multi-Layered Metallic Films. Key Engineering Materials, 2007, 353-358, 1863-1866.	0.4	0
537	Study of the Tensile Strength of Nanostructured Copper Obtained by Electrodeposition and SMAT. , 2007, , 455.		0
538	Preparation and capacitance behavior of nickel oxide-titania nanocomposite. , 2007, , .		0
539	Bioactive modification of NiTi shape memory alloy. , 2007, , .		0
540	Contribution of the Experimental Mechanics to the Automotive Design. , 0, , .		0

#	Article	IF	CITATIONS
541	Experimental and FEA Investigations on the Fracture Properties of Pipe Structures Under Internal Pressure in DBTT Region. Journal of Pressure Vessel Technology, Transactions of the ASME, 2009, 131, .	0.6	0
542	Comparison of Surface Nanostructured Electrodeposited Cu Produced from Different Power Types: Microstructure and Tensile Properties. Materials Science Forum, 2009, 614, 189-196.	0.3	0
543	Experimental Evaluation of the Size Effect on the Ductile and Brittle Fracture Toughness of a Steel Pressure Vessel. Materials Science Forum, 2009, 614, 41-46.	0.3	0
544	Nanostructured 316 Stainless Steel Prepared under Traction by Surface Mechanical Attrition Treatment. Materials Science Forum, 2009, 614, 201-206.	0.3	0
545	A Computational Study of Plastic Deformation in AISI 304 Induced by Surface Mechanical Attrition Treatment. , 2010, , .		0
546	Damage Analysis of Tensile Deformation of Co-rolled SMATed 304SS. , 2010, , .		0
547	Investigation of an Updated Continuum Damage Model in the DBTT Region. , 2010, , .		0
548	Surface hardening of NiTi shape memory alloy induced by surface nanocrystallization via surface mechanical attrition treatment. , 2010, , .		0
549	Investigation of the Hydrogen Embrittlement on the 65Mn Steel from the Nuclear Power Plant with Small Punch Method. Advanced Materials Research, 2010, 118-120, 206-210.	0.3	0
550	Characterization of plastically graded nanostructured material. , 2010, , .		0
551	Preface: Special Issue of Materials and Manufacturing Processes: "Surface Engineering― Materials and Manufacturing Processes, 2010, 25, 287-287.	4.7	0
552	Oxidation Behavior of Cu-38at%Zn Foils After Surface Mechanical Attrition Treatment. Corrosion, 2012, 68, 035003-1-035003-7.	1.1	0
553	Investigating the Humidity Effect on Si/PEDOT:PSS Hybrid Solar Cell and Power Conversion Efficiency Recovery by Re-Deposition of the Hole Transporting Layer. , 2013, , .		0
554	Growth behaviors of ZnO nanostructure on SMAT Cu _{0.62} Zn _{0.38} during oxidation. EPJ Applied Physics, 2013, 62, 20401.	0.7	0
555	Behavior Identification of a Multi-Layered Graded Stainless Steel Using an Inverse Method. Key Engineering Materials, 2014, 626, 85-90.	0.4	0
556	Investigation of Controllable Parameters of Mechanical Treatment on Aluminum-Based Composite in Marine Application. Materials Science Forum, 0, 813, 307-314.	0.3	0
557	Numerical Simulation of Ballistic Performance of Nanocrystalline and Nanotwinned Ultrafine Crystal Steel. Materials Science Forum, 0, 813, 285-292.	0.3	0
558	Parameter Study of Numerical Simulation for Tensile Properties of Multi-Layer SMATed Alloys. Materials Science Forum, 0, 813, 293-299.	0.3	0

#	Article	IF	CITATIONS
559	Black TiO ₂ Nanomaterials Through Electrochemical and Mechanical Methods. , 2017, , 33-47.		0
560	Low Cost Structural Morphing AUV for Long-term Water Column Exploration and Data-harvesting. , 2018, , .		0
561	Surface mechanical attrition treatment of commercially pure titanium by electromagnetic vibration. International Journal of Materials Research, 2019, 110, 963-968.	0.3	0
562	Theoretical and experimental study of bistable symmetric shells built by locally nanostructuring an isotropic plate. IOP Conference Series: Materials Science and Engineering, 2019, 531, 012018.	0.6	0
563	Numerical and experimental comparison of two nano-structuring processing techniques on making stronger stainless steels. Materials Today Communications, 2020, 24, 100419.	1.9	0
564	A Selfâ€Supported Highâ€Entropy Metallic Glass with a Nanosponge Architecture for Efficient Hydrogen Evolution under Alkaline and Acidic Conditions (Adv. Funct. Mater. 38/2021). Advanced Functional Materials, 2021, 31, 2170283.	14.9	0
565	Braking Force Model on Virus Transmission to Evaluate Interventions Including the Administration of COVID-19 Vaccines — Worldwide, 2019–2021. China CDC Weekly, 2021, 3, 869-877.	2.3	0
566	Evaluation of Damage and Plastic Properties by Microindentation and Inverse Method. , 2007, , 139-140.		0
567	Use of Instrumented Microindentation to Determine the Global Mechanical Behavior of Nanocrystallised Copper Samples. , 2007, , 543-544.		0
568	Integrated Design for Fatigue Life Estimation of Structures. Strojniski Vestnik/Journal of Mechanical Engineering, 2011, 7-8, 547-554.	1.1	0
569	Study on Mechanical Properties of 2024 Al Sheet Treated by Smat and Hot/Cold Rolling. , 2012, , 239-244.		0
570	Residual Stress Evaluation of Materials Manufactured by High-Energy Process. , 1990, , 303-312.		0
571	Etude du comportement et de l'endommagement des composites à matrice aluminium et à renforts particulaires. European Physical Journal Special Topics, 1993, 03, C7-1867-C7-1871.	0.2	0
572	Ballistic Performance of Bimodal Nanostructured and Nanotwin-Strengthened Metals. , 2018, , 205-224.		0
573	Tooling Design and Fatigue Life Evaluation via CAE Simulation for Metal Forming. , 2008, , 711-720.		0
574	Simulation-Enabled Approach for Defect Prediction and Avoidance in Forming Product Development. , 2008, , 3-12.		0
575	Aerodynamic Performance of a Nanostructure-Induced Multistable Shell. Aerospace, 2021, 8, 350.	2.2	0
576	Low-temperature plasma nitriding of AISI 304 stainless steel with nano-structured surface layer. International Journal of Materials Research, 2022, 94, 1143-1147.	0.3	0